8. Lilly, John C., Victor Legallais and Ruth Cherry. 1947. "A Variable Capacitor for Measurements of Pressure and Mechanical Displacements: A Theoretical Analysis and Its Experimental Evaluation." J. Appl. Phys. 18 :613-628

Double Sides

A Variable Capacitor for Measurements of Pressure and Mechanical Displacements; A Theoretical Analysis and Its Experimental Evaluation

JOHN C. LILLY, VICTOR LEGALLAIS, AND RUTH CHERRY

Reprinted from JOURNAL OF APPLIED PHYSICS, Vol. 18, No. 7, pp. 613–628, July, 1947

Reprinted from JOURNAL OF APPLIED PHYSICS, Vol. 18, No. 7, 613–628, July, 1947

A Variable Capacitor for Measurements of Pressure and Mechanical Displacements; A Theoretical Analysis and Its Experimental Evaluation*

JOHN C. LILLY, VICTOR LEGALLAIS, AND RUTH CHERRY
E. R. Johnson Foundation for Medical Physics, University of Pennsylvania, Philadelphia, Pennsylvania
(Received December 13, 1946)

A variable capacitor is described for measuring (1) small displacements, (2) small volume changes, and (3) pressure differences. The capacitor consists of a deflectable diaphragm and a fixed electrode. The diaphragm is metallic, plane-parallel, clamped at the edges, and at ground potential; the electrode, at an a.c. potential, has a plane surface parallel to the undeflected plate across an air gap. For use in displacement measurements, the diaphragm's center is deflected by a point contact from a mechanical link to the observed system, or by a uniform pressure load from a fluid link to the system. The fluid link is used also when measuring volume changes and pressure differences. The plate deflection results in a change in the air gap, and thus generates a capacitance signal. This signal is measured by electrical methods.

A theoretical analysis of this variable capacitor is presented; sensitivity and alinearity factors for the three uses of the device are derived. The experimental performance shows reasonably satisfactory agreement with the derived theory. The displacement of the plate's center was measured with an interferometric method, using a yellow He line as a standard of reference; the applied pressure, with a liquid manometer; and the capacitance signal, with a standard capacitor substitution procedure. The gauge can be used so as to give quantitative electrical indications of displacement, volume change, or pressure difference; or can be used as a null indicator device in which an unknown pressure is balanced against a known one on opposite sides of the diaphragm. In order to achieve large volume an displacement sensitivities, small air gaps (5.10^{-4} cm) are employed. Details of a construction method to assure small values are presented.

INTRODUCTION

TO anyone who has attempted the design or the construction of a diaphragm capacitance gauge for precise pressure or volume-change measurements, the lack of an adequate theory to handle the many variables encountered is rather discouraging. The important variables are the diaphragm diameter, thickness, and material; the air gap, the electrode diameter, the applied pressure, and the capacitance signal. The magnitude of the pressure signal and the desired capacitance signal are known. But what about the values to be assigned the first five variables in order to achieve the desired pressure-capacitance relation? It was an attempt to answer this question that led to this analysis.

Though the theory presented here was evolved in response to a need in the biological field, the treatment and the results are sufficiently general to be of interest to the physicist, the chemist, or the engineer who may want a gauge for other applications. For the benefit of those who may apply the gauge to biological systems, and for the benefit of those interested in why biological applications are as strict in their requirements as the physical ones, the peculiarities of the living systems are presented and discussed in relation to the capacitor gauge design. For those interested only in gauge design, this discussion on biological problems may be neglected, and a start made on the later, theoretical derivation section.

THE GAUGE DESIGN PROBLEM IN BIOLOGICAL APPLICATIONS

The pressure gauge design problems encountered in the biological field are different from those in other fields of research. Certain limitations are placed on the pick-up unit design by the special properties of animals. In general, the pressure systems in animals are buried within the body, loosely supported, of variable distensibility, in constant motion, and are fragile in construction. These structures react locally to probing, puncturing, and tearing by bleeding and by constricting. Blood in the vessels may clot on inserted objects, and thus plug pressure taps. The whole animal also reacts by moving and by markedly changing the blood pressure, the heart rate, and other variables one may be measuring. Anesthetics can be used to abolish many of these undesired effects; but these drugs can exert other actions which are also unwanted.

* The work described in this paper was done under a contract recommended by the Committee on Medical Research, between the Office of Scientific Research and Development and the University of Pennsylvania.

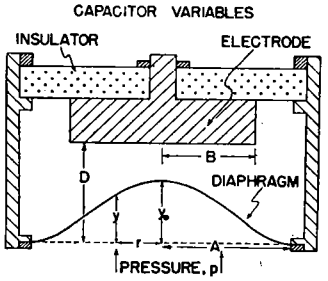

FIG. 1. Diagram of a diaphragm capacitor. The variables used in developing the capacitor theory are illustrated here; capital letters refer to fixed geometrical properties, small letters to variables generated by a displaced diaphragm. Tables I and II give the definitions and the units of all variables. The diaphragm is shown in an approach deflection; in a recession deflection the diaphragm would bulge downward. Both the air gap and the center deflection are greatly magnified in relation to the diameters of the diaphragm and of the electrode. The form of the deflected diaphragm is that of a stiff, edge-clamped plate; Figs. 2 and 3 give quantitative details of the two extreme idealized diaphragm forms assumed in the theory.

The pressure phenomena occurring in animals have both a static level and superimposed rapid pulsations. It is important to record these phenomena faithfully.

Because of these special properties of the animal, some form of transmission of the pressure signal from the interior to the exterior is necessary. At the present time, tubing containing liquid usually conducts the signal; ultimately, electrical transmission may be substituted. To avoid undesired local stimuli, the tubing is small.

From these considerations, some requirements for a pressure gauge pick-up can be deduced. (1) The pick-up must reproduce static level signals. (2) For the faithful reproduction of rapidly changing pressures transmitted through small bore tubing, and to minimize the length of the tube bore exposed to coagulable blood, the volume change of the unit with respect to an applied pressure must be minimal. (3) The pick-up size and the weight should be as small as possible. (4) The connection between the pick-up unit and the recorder must be long and very flexible. (5) The pick-up and its leads should be insensitive to vibration and to changes in position.

Many types of diaphragm pressure gauges have been used in recording static and kinetic pressures in animals.[1–8] The ones with the greatest promise of meeting the above requirements are the photoelectric[6,7] and the electrical capacitor[8] types. The latter type is the one analyzed here.

With the above conditions in mind, it was considered important to examine the theoretical basis of the pick-up unit of a diaphragm-type capacitor pressure gauge previously applied to the recording of pressure in the vascular system.[8] The examination, presented below, was undertaken in order (1) to find out what factors were of importance in an optimal design for a pick-up unit for a minimal volume change and maximal capacitance signal in response to a given applied pressure; (2) to facilitate making design compromises in the presence of construction difficulties in special units; (3) to find and to evaluate those factors in the design which determine the alinearity and the sensitivity of the gauge; and (4) to explain and thus make allowances for the observed differences in gauge

TABLE I. Measured and calculated variables for a given gauge.

I. Measured variables	Units	Method
1. Electrode radius	B cm	
2. Diaphragm radius	A cm	By micrometer
3. Diaphragm thickness	T cm	
4. Applied pressure	p dynes/cm²	By liquid manometer
5. Central point deflection, at p	y_0 cm	By interferometer
6. Displaced volume, at y_0	v cm³	By calibrated capillary
7. Gauge capacitance, at $y_0=0$	C_0 cm	By substitution for standard condenser in an electrical circuit
8. Capacitance signal, at y_0	c cm	
II. Calculated variables, as derived from measured ones		
9. Air gap, at $y_0=0$	D cm	$D=B^2/4C_0$
10. Displaced volume, at y_0	v cm³	$v=(y_0)(\pi/k)A^2$
11. Relative deflection	w (0)	$w=y_0/D$
12. Radius ratio, squared	N (0)	$N=(B/A)^2$
13. Relative capacitance signal	s (0)	$s=c/A^2/4D=(c/C_0)N$
14. Deflection constant, stiff	K cm²/dyne	$K=(y_0/p)(T^3/A^4)$ $K=\frac{3}{16}(1-t^2)/Y$ (t=Poisson's ratio; Y=Young's modulus)
15. Deflection constant, flexible	$1/G$ cm/dyne	$1/G=(y_0/p)/A^2$
16. Volume constant, stiff	k (0)	$k=y_0(\pi A^2)/v=3$
17. Volume constant, flexible	k (0)	$k=y_0(\pi A^2)/v=2$
18.	H (0)	$H=(1-N)$
19.	u (0)	$u=w^2$
III. Calculated variables, as related in theory: see equations in Table III		

[1] O. Franck, Zeits. f. Biol. **82**, 49 (1925).
[2] C. J. Wiggers, J. Lab. and Clin. Med. **10**, 54 (1924).
[3] W. F. Hamilton, Am. J. Physiol. **107**, 427 (1934).
[4] A. Hampel, Pflunger's Arch. Ges. Physiol. **244** (2), 171 (1940).
[5] W. G. Kubicek, Rev. Sci. Inst. **12**, 101 (1941).
[6] H. Rein, Arch. f. d. Ges. Physiol. **243**, 329 (1940).
[7] W. E. Gilson, Science **95**, 514 (1942).
[8] J. C. Lilly, Rev. Sci. Inst. **13**, 34 (1942).
[8a] F. Buchthal and E. Warburg, Acta Physiol. Scandinavica **55**, 55–70 (1943).

TABLE II. Sensitivity and alinearity factors for a constant B/A and a given w.

I. Sensitivity factors	Secant form	Tangent form	Initial value, $y_0 \to 0$
20. Relative displacement	$m = s/w$	$n = (\partial s/\partial w)$	$M = (1-H^k)/k$
21. Displacement	$c/y_0 = (m/4)(A/D)^2$	$\partial c/\partial y_0 = (n/4)(A/D)^2$	$S_y = (M/4)(A/D)^2$
22. Volume	$c/v = km/4\pi D^2$	$\partial c/\partial v = kn/4\pi D^2$	$S_v = kM/4\pi D^2$
23. Pressure	$c/p = mKA^6/4T^3D^2$	$\partial c/\partial p = nKA^6/4T^3D^2$	$S_p = MKA^6/4T^3D^2$
23a. Pressure	$c/p = (c/y_0)(y_0/p)$	$\partial c/\partial p = (\partial c/\partial y_0)(\partial y_0/\partial p)$	$S_p = (M/4)(A/D)^2(y_0/p)$
II. Alinearity factors			
24. Relative displacement	$a = m/M$	$b = n/M$	$a = b = 1.00$
25. Displacement	$a_d = (c/y_0)/S_y = a$	$b_d = (\partial c/\partial y_0)/S_y = b$	$a_d = b_d = 1.00$
26. Volume	$a_v = (c/v)/S_v = a$	$b_v = (\partial c/\partial v)/S_v = b$	$a_v = b_v = 1.00$
27. Pressure	$a_p = (c/p)/S_p = a$	$b_p = (\partial c/\partial v)/S_p = b$	$a_p = b_p = 1.00$

TABLE III. Theoretical equations relating s, w, and B/A.*

Stiff plate (Fig. 2)		Flexible membrane (Fig. 3)	
		Approach case	
(2.0)	$s = (1/u)\tanh^{-1}[uN/(1-wH)] - N$	(2.1)	$s = (1/w)\ln[(1-wH)/(1-w)] - N$
(3.0)	$s = [(\frac{1}{3})(1-H^3)w + (\frac{1}{5})(1-H^5)w^2 + \cdots]$	(3.1)	$s = [(\frac{1}{2})(1-H^2)w + (\frac{1}{3})(1-H^3)w^2 + \cdots]$
(4.0)	$n = (\frac{1}{2})[1/(1-w) - H^3/(1-wH^2) - m]$	(4.1)	$n = 1/(1-w) - H^2/(1-wH) - m$
		Recession case	
(5.0)	$s = (1/u)\tan^{-1}[uN/(1+wH)] - N$	(5.1)	$s = (1/w)\ln[(1+w)/(1+wH)] - N$
(6.0)	$s = [-(\frac{1}{3})(1-H^3)w + (\frac{1}{5})(1-H^5)w^2 - \cdots]$	(6.1)	$s = [-(\frac{1}{2})(1-H^2)w + (\frac{1}{3})(1-H^3)w^3 - \cdots]$
(7.0)	$n = (\frac{1}{2})[1/(1+w) - H^3/(1+wH^2) - m]$	(7.1)	$n = 1/(1+w) - H^2/(1+wH) - m$

* Note that (Table I): $u^2 = w$; $N = (B/A)^2$; $H = (1-N)$.
The variables are defined in Figs. 1, 2, and 3, and in Table I. (1) Fundamental integral: $s = [(4D/A^2)\int_0^B (rdr)/2(D \pm y)] - N$. Solutions: [from (1) and equations of Figs. 2 and 3].

performance in the case in which the diaphragm is deflected away from the electrode in contrast to the case of diaphragm-electrode approach.

In addition to the measurement of pressure, a diaphragm-type capacitor has desirable characteristics for use as an ultramicrometer (displacement) and as a dilatometer (volume change). In the theory below, the condenser characteristics for these three uses are most easily discussed in the order: displacement, volume, and lastly, pressure. (In the theory, displacements are considered only as measured by means of a fluid link; in practice, point contact mechanical links can be used, but this theory does not apply in this case, even with a stiff plate.)

The following sections give a summary of a derivation of a diaphragm capacitor theory, and some applications of the theory in the design and in the testing of diaphragm capacitors. Later sections deal with the results of an experimental check of the theory, a consideration of electrical circuits for recording with the gauge, and a method used in the construction of some pick-up units.

DERIVATION OF A THEORY OF A DIAPHRAGM-TYPE CONDENSER

A. Configuration of the Capacitor

In deriving a theory of a diaphragm-type capacitor an expression is first developed which relates the displacement of the diaphragm to the resultant capacitance signal, for the geometrical arrangement shown in Fig. 1. In the following discussion, variables generated by a diaphragm deflection are represented by small letters, and the constants of a given gauge, by capital letters (see also Tables I and II).

The diaphragm is a circular plane-parallel metal plate or membrane clamped near the periphery and is assumed to be deflected by a uniform pressure load on one side or the other. The effective radius of this diaphragm, A, is that of the periphery at the inside edge of the clamp.

The electrode is a circular metal structure with a plane surface placed parallel to the undeflected plate, across an interposed air gap of a thickness D. The effective electrode radius, B,

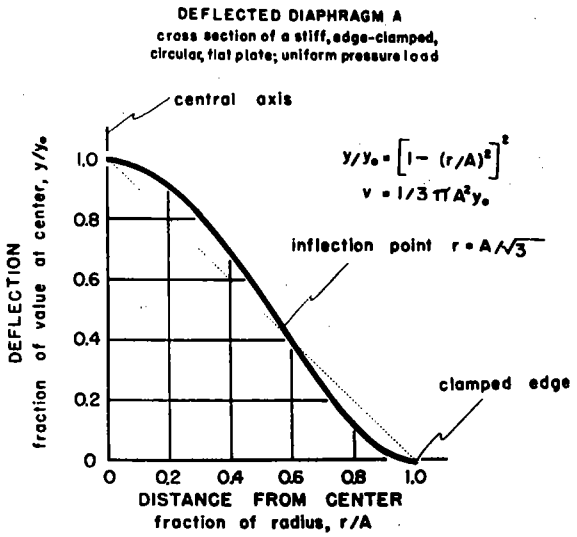

FIG. 2. The form taken by a stiff plate deflected by a uniform pressure. A radial section is cut through the diaphragm, from the axis of rotation at the left, to the clamped edge at the right. This method of showing the form greatly magnifies the amount of the deflection in relation to the radius by a factor of about one to ten thousand. The equation of this curve is derived on the assumptions that the absolute deflection is less than about 1/50 the thickness of the diaphragm, that the thickness is less than about 1/50 of the radius, and that the edge is uniformly and rigidly clamped, without exerting a radial tension in the undeflected position of the diaphragm (no initial stretching). All strains are assumed to be within the proportional elastic limit. It is further assumed that, in the undeflected state, the diaphragm is a plane, parallel, homogeneous, and isotropic structure. The equation of this curve is given in the figure; the variables are defined by Fig. 1. The volume swept out by the diaphragm as it is deflected, v, was found by integration of the equation for the curve; the resulting expression gives the dimensions of a cone of equivalent volume.

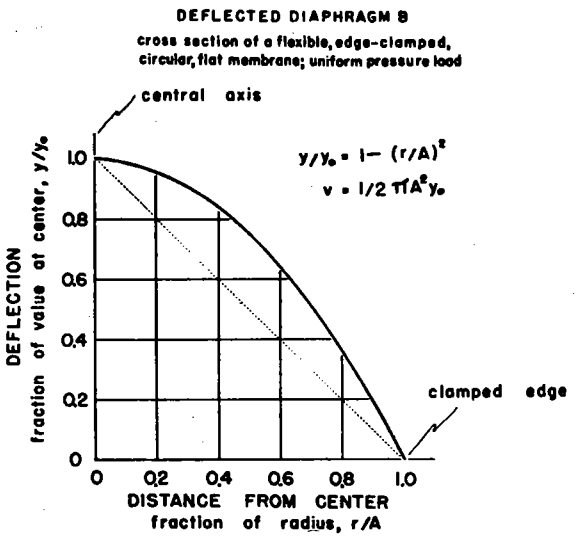

FIG. 3. The form taken by a flexible membrane deflected by a uniform pressure. The general statements made under Fig. 2 apply to this figure. The same limiting assumptions apply to this equation as to the stiff-plate one, except that it is assumed that the membrane is subjected to a uniform tension of $G/4$ cm/dyne (item 15, Table II) in all directions in its own plane in the undeflected state. In this diaphragm the inherent stiffness is assumed to be negligible, and hence the clamped periphery bends with a practically infinitesimal radius of curvature. The volume swept out by the diaphragm as it is deflected, v, equals that of a cylinder of a height equal to one-half the central deflection and a base of an area equal to that of the undeflected diaphragm.

is that of the plane surface presented to the air gap.

The diaphragm and the electrode have a common axis passing through their centers, normal to their facing surfaces (Fig. 1).

Since the ratio of the electrode periphery to the air-gap thickness, $2\pi B/D$, is usually of the order of magnitude of 750–7500; edge effects are considered to be negligible and are omitted in the following analysis.

B. Derivation Summary

An equation defining the relation of the relative change in capacitance of this capacitor to the deflection of the diaphragm (Fig. 1) can be derived in the following manner:

1. Consider an elemental capacitor consisting of an annulus of infinitesimal width, lying in the surface of the electrode and concentric with the central axis, and of a similar strip directly across the air gap, lying in the surface of the diaphragm. Let both strips have a radius of r, defined as the distance along a normal from the annulus to the axis. Assume that, as the plate is moved by a pressure load, the capacitance of this elemental capacitor, dc, (in centimeter units) varies inversely with the distance between the strips, and varies directly with the area of one strip ($2\pi r dr$) (Eq. (1), Table III, note).

In the usual case, the deflection of the diaphragm center is only about 1/500 to 1/5000 of the diaphragm radius; therefore it can be shown that the above assumption is justified.

2. Consider the annular element in the surface of the diaphragm in the deflected position. The displacement of this element from the undeflected position is taken as y, and that of the diaphragm center as y_0. The relation between the radius of the annulus, r, and y, should be con-

sidered for at least two extreme cases, the thin, stiff plate and the thin, flexible membrane.[9]

The equation relating y, y_0, r, and A for the stiff plate is given in Fig. 2; and that for the flexible membrane in Fig. 3. (These equations are taken from Love's *The Mathematical Theory of Elasticity*, and reference 9.) The equations are exact only for values of y_0/A which are very small compared with unity. Other assumptions and limits for these equations are given in the Figs. 2 and 3 captions.

3. By setting up the differential equation implied in assumption 1 above, substituting the expression for assumption 2, for the two diaphragm types and integrating the result, the equations of Table III can be derived. These equations, in Table III, state the relation between the relative capacitance signal, s, and the relative change in the air gap, w (equals y_0/D). In these expressions the parameter is the electrode-diaphragm radius ratio, B/A. All of the deflections of the diaphragm toward the electrode are treated as the "approach case," and deflections away from the electrode as the "recession case."[10] The equations of these two cases differ fundamentally only in the algebraic sign of the central diaphragm displacement term, y_0, which is positive in recession and negative in approach.

For calculation purposes, the arc tangent, the arc hyperbolic tangent, and the logarithmic forms of the solution were used for numerical values of y_0/D greater than 0.10, and the series forms for the lesser values (0.00 to 0.10).

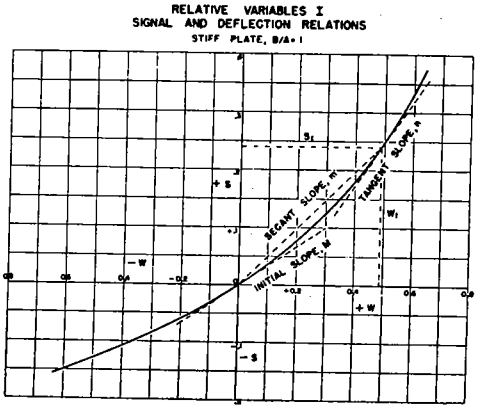

FIG. 4. Relation between the relative displacement and the relative capacitance change for a stiff plate. This curve is for an electrode and a stiff plate diaphragm (Fig. 2) of equal radii. For any condenser with a given radius ratio, B/A (Fig. 1), the fractional, or relative, capacitance change, s, is defined as the capacitance change, c, divided by the undeflected state capacitance, C_0, of a condenser with a B/A of unity and the same initial air gap, D (Fig. 1 and item 13, Table I). The fractional air-gap change or the relative displacement, w, is defined as the central diaphragm deflection, y_0, divided by the air gap, D, in the undeflected state (Fig. 1). This figure serves to define the relative displacement sensitivities, M, m, and n in terms of the slopes of the s and w curve. The secant m, and the tangent n, are both defined at any point on the curve, s_1 and w_1; the initial slope, M, is that at the origin, $s=w=0$. The sole dependence of the initial slope, M, on the radius ratio, B/A, is shown in the next figures. Both m and n approach M as the deflection, w, becomes infinitesimal. For the assumptions and the theory of this curve see text. It is to be noted that the variables used in this and in most of the rest of the figures have zero dimensions.

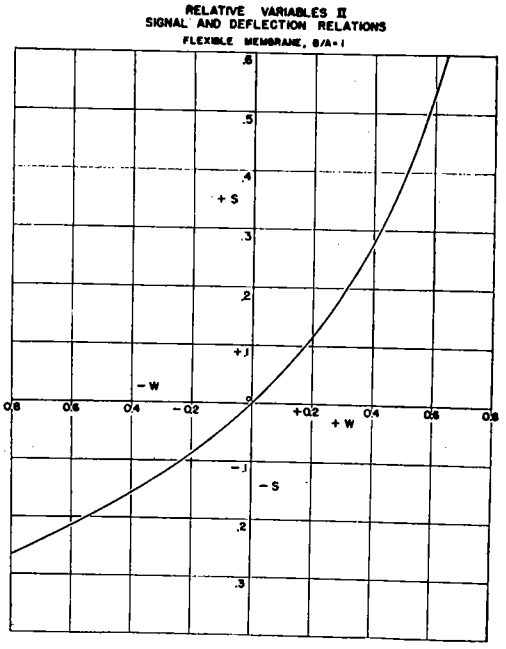

FIG. 5. Relation between the relative displacement and the relative capacitance change for a flexible membrane. The figure is the same as Fig. 4 with the exception that the diaphragm here is a flexible membrane (Fig. 3) instead of a stiff plate. The definitions of the variables are given under Fig. 4; the theory is developed in the text.

USE OF THE THEORY IN THE DESIGN OF PICK-UP UNITS

A. Factors Influencing the Sensitivity

In general the final objective in a problem of the design of a pick-up unit is reached when the unit produces a capacitance signal of the mag-

[9] I. B. Crandall, *Theory of Vibrating Systems and Sound* (D. Van Nostrand Company, New York, 1927).

[10] Roess gives a stiff plate approach case equation which is equivalent to the inverse hyperbolic tangent function in Table III. [L. C. Roess, Rev. Sci. Inst. 11, 183 (1940).]

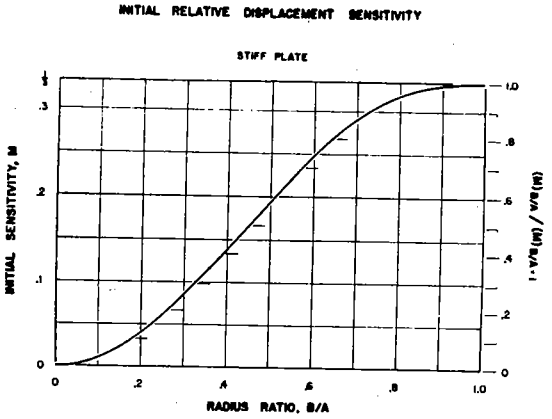

FIG. 6. The dependence of the initial relative displacement sensitivity on the radius ratio for a stiff plate. As is shown in the theory in the text, the initial relative displacement sensitivity, M (Fig. 4), is a function solely of the radius ratio, B/A (Fig. 1). The right-hand scale shows the sensitivity at a given B/A as a fraction of that at the maximum value, at B/A of unity. The initial absolute sensitivity, defined as the absolute capacitance change, c, divided by the absolute central deflection, y_0 (Fig. 1), can be calculated from these values of M, the electrode radius B, the diaphragm radius A, and the initial air gap, D (see text). The ratios of the secant, m, and the tangent, n, relative sensitivities (Fig. 4) to M for a number of radius ratios is shown in later figures.

nitude required by a chosen electrical circuit in response to an applied displacement, volume, or pressure change of a size determined by the system in which measurements are to be made. In other words, the designer's problem is to achieve a definite gauge sensitivity. In most biological applications to pressure recording, as was shown above, an additional part of the final objective is to have the volume of the gauge change a minimal amount. In some applications, a minimal alinearity of the calibration curve is also desirable.

Two useful types of sensitivity factors can be defined for diaphragm gauges; the absolute and the relative types. The absolute factors are defined in terms of the variables measured while the gauge is in use, which are the displacement, the volume, or the applied pressure, and the resulting capacitance signal. The relative sensitivity factors are expressed in terms of dimensionless quantities, such as those used in the theoretical equations developed above. After the gauge constants are known, the absolute sensitivity factors can be calculated from the relative sensitivity ones. This calculation will be dealt with in a later section.

B. Relative Sensitivity

Figures 4 and 5 show the graphs of the function relating the relative capacitance signal, s, to the relative displacement factor, y_0/D, for a radius ratio, B/A, of 1.00 (Tables I and III). As the plate or membrane deflects an infinitesimal amount in either direction (y_0/D approaching zero), the slope of this curve has a definite value. From inspection of the series forms of the equations in Table III, it can be seen that this slope at the origin is a function only of the radius ratio, B/A; this slope is called the "initial relative displacement sensitivity," M, for a given value of the radius ratio, B/A. Figures 6 and 7 show the relation between M and B/A for the two extreme diaphragm types.

As the relative displacement, w (equal to y_0/D, Table I), increases beyond an infinitesimal value, the relative sensitivity changes from the initial value, M. Two useful types of relative sensitivity factor can be defined for the rest of the curve; these two types are illustrated in Fig. 4. The slope of a straight line from any point on the

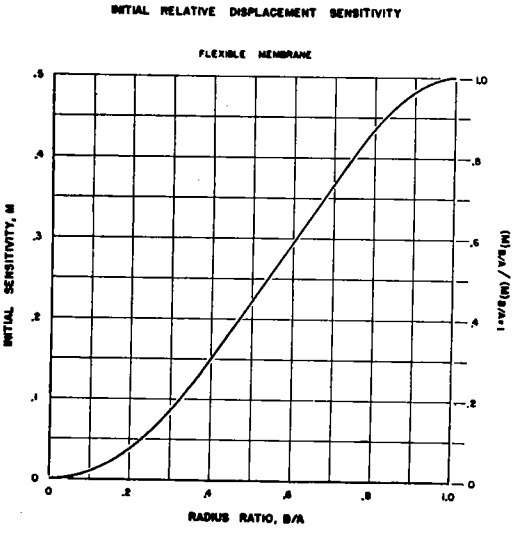

FIG. 7. The initial relative displacement sensitivity and the radius ratio for a flexible membrane. The statements under Fig. 6 apply also to this figure. It is to be noted that the maximum value of M at a B/A of unity for the flexible membrane is one-half, and that for the stiff plate (Fig. 6) is one-third. From the expression for the initial absolute volume sensitivity, S_v, (item 22, Table II), and these values of M and the volume constant, k (16 and 17, Table I), it can be shown that the initial absolute volume sensitivity for the stiff plate is equal to that of the flexible membrane considering all other geometrical values as identical, and B/A as unity.

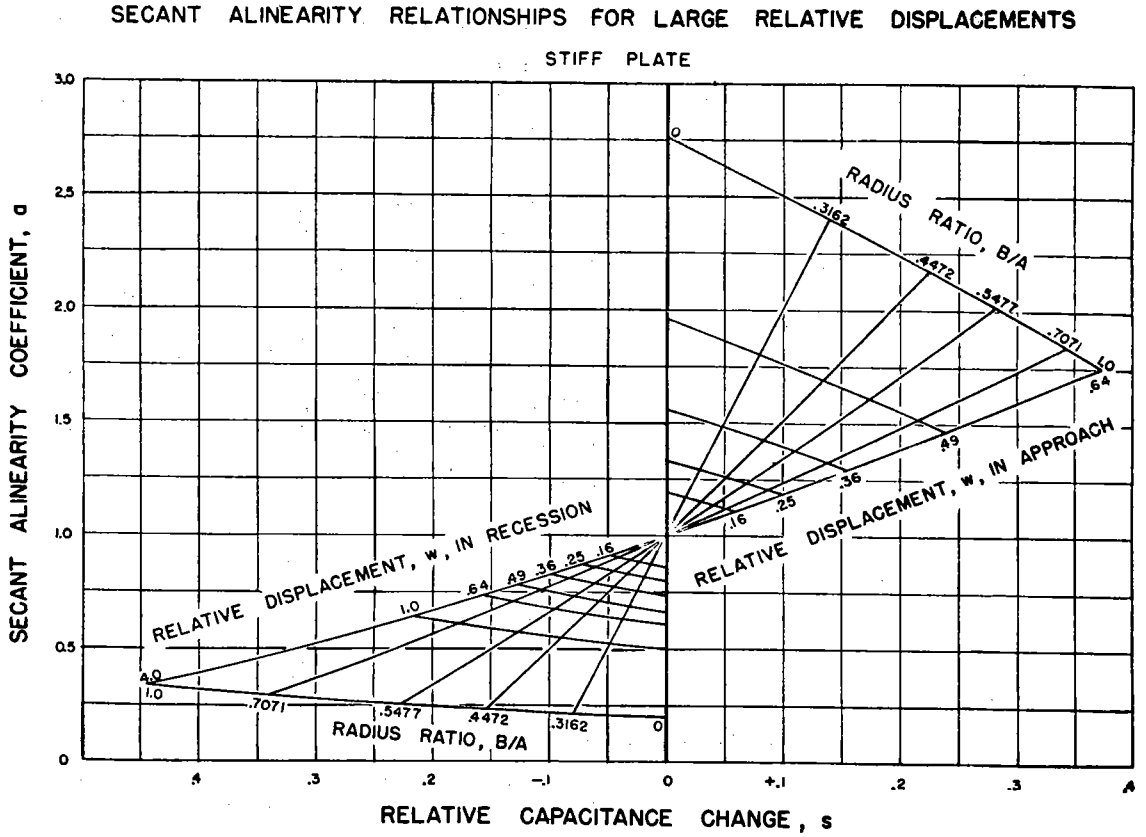

FIG. 8. The secant alinearity coefficient and the relative capacitance signal relations for a stiff plate for large relative deflections. Some of the variables used in this graph are defined under Fig. 4, all variables are defined in Tables I and II. The secant alinearity coefficient, a, is the ratio of the secant relative displacement sensitivity, m, to the initial displacement sensitivity, M. This figure shows the dependence of a on B/A, s, and w for a stiff plate. A point to be noted is the large deviations from linearity in the approach condition as contrasted with the smaller deviations in recession, for corresponding values of w.

curve to the origin is called the "secant relative sensitivity," m, which is equal to s/w, Table I.

The slope of the curve itself at the same point is the "tangent relative sensitivity," n, which is equal to $\partial s/\partial w$. Both m and n approach the initial relative sensitivity value, M, as the relative displacement approaches zero, this property of these functions provides a convenient definition for two useful alinearity coefficients.

C. Gauge Alinearity

Two alinearity coefficients, a and b, can be derived from the two displacement sensitivity factors, m and n. The "secant alinearity coefficient," a, is defined as the ratio of the secant sensitivity to the initial sensitivity, m/M, and the "tangent alinearity coefficient," b, as n/M. Both of these coefficients are defined for a constant value of the radius ratio, B/A, and are a function of w.

These two coefficients have the value of 1.00 as the relative displacement of the diaphragm approaches zero, i.e., a capacitor gauge is most linear for those diaphragm deflection values which are a very small fraction of the air gap value. This relation is true for the opposite cases of recession and approach, for both types of diaphragm; in recession, the coefficient values are less than 1.00; in approach, greater than 1.00. Figures 8 through 13 show these relations between a, b, s, w, and B/A for the two diaphragms.

If the displacement of the center of the diaphragm, y_0, is a linear function of the volume change, v, or of the applied pressure, p, both coefficients give the alinearity values for actual

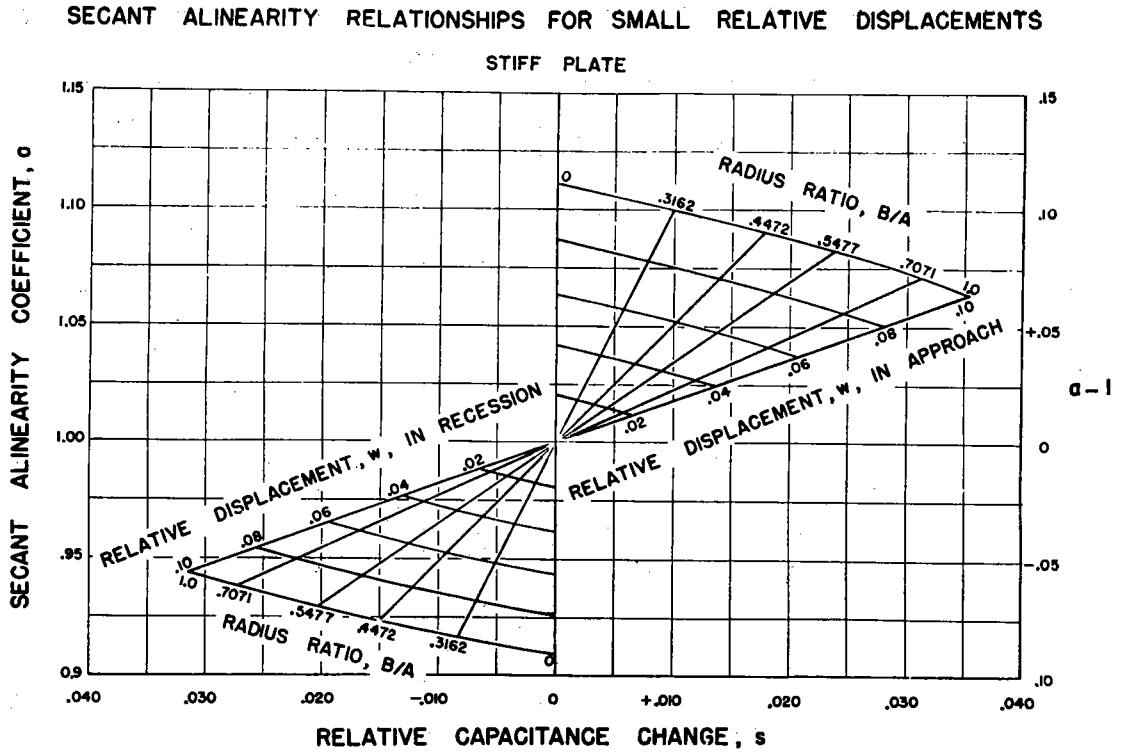

FIG. 9. The secant alinearity coefficient relationships for a stiff plate for small values of the relative displacement. This figure is an amplification of the part of Fig. 8 near zero capacitance change. In those uses of the gauge requiring a high degree of linearity, the variables are restricted to the range on this plot or to an even smaller range. The considerations mentioned under Fig. 8 apply also to this figure.

volume and pressure gauges. In other words, for a constructed gauge the ratio of the slope of the volume change-capacitance curve, or of the pressure-capacitance curve at a given pressure or volume, to the initial slope is given directly by the value of the alinearity coefficients at a given s, the relative capacity signal for a given radius ratio, B/A. A mechanical design which has a fairly linear pressure-deflection relation is discussed in the section on experimental performance.

D. Absolute Types of Sensitivity

The absolute sensitivity factors are divided into the two general types, secant and tangent, defined above for the relative displacement factors.

It is convenient to define each of the secant factors as the ratio of the capacitance signal, c, to the displacement, y_0, to the volume, v, or to the pressure, p. The tangent sensitivities are defined as the rate of change of the capacitance with respect to each of the three variables. All of these absolute factors are calculable from the gauge constants, A, B, D (or C_0) and the corresponding relative displacement sensitivities, m and n; however, it may be easier to use these constants, the initial relative displacement sensitivity, M, and the two alinearity coefficients, a and b. The equations for these calculations are given in Table II.

The absolute displacement sensitivity, (c/y_0), for a given value of B/A, can be shown to be equal to one-fourth the product of the square of the ratio of the diaphragm radius to the air gap, $(A/D)^2$, and the relative sensitivity, M (Table II); c/y_0 has an initial value of $(c/y_0)_0$ when m equals M. The corresponding tangent factor, dc/dy_0, is similarly calculable by substitution of n for m (Table II). The values of a for these and later calculations for various values of B/A and w are given in Figs. 8, 9, and 10; the b values, in Figs. 11, 12, and 13.

In other words, the absolute displacement

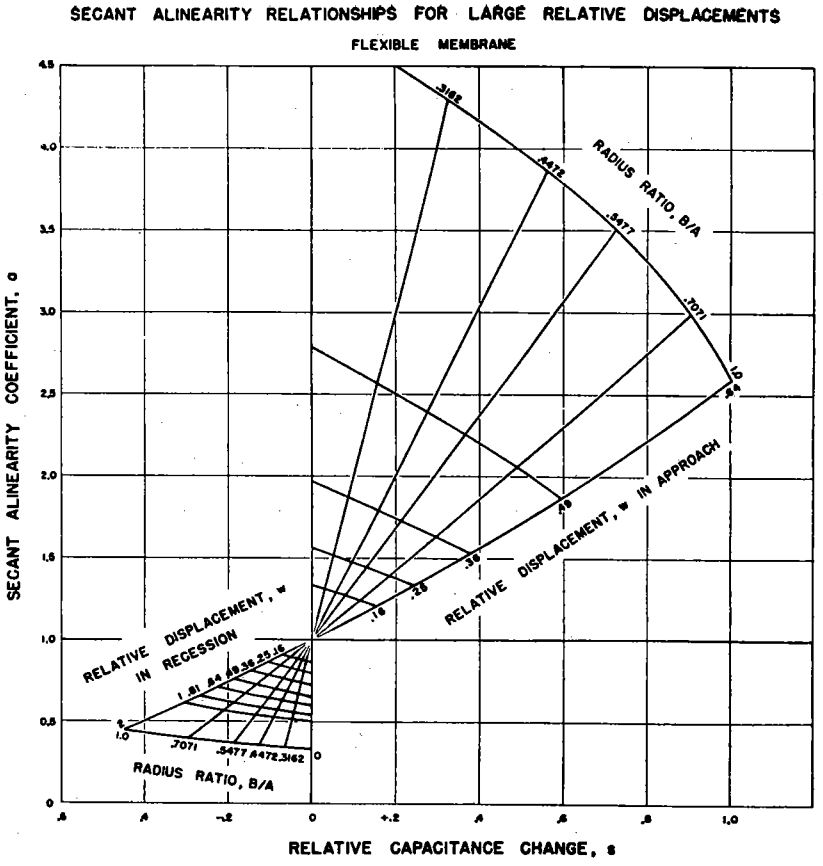

FIG. 10. The secant alinearity relationships for a flexible membrane. This plot for a flexible membrane is of the same type as the one for the stiff plate shown in Fig. 8. Comparing this figure with number 8 it can be seen that the flexible membrane has greater deviations from ideal linearity (a equal to 1.0) than does the stiff plate for the same value of the relative displacement, w.

sensitivities, secant and tangent, are independent of the absolute values of the diaphragm radius, thickness, and material; of the electrode radius; and of the air gap. However, these factors are dependent on the ratio of the diaphragm radius to the air gap, and on the relative displacement sensitivity.

The absolute volume sensitivity factors, for a given value of B/A are calculable by the equations given in item 22, Table II; or as in the case of c/y_0, by the substitution of M and a or b, for m or n in the equations. By these equations it can be shown that the two absolute volume sensitivities for both diaphragm types are independent of the absolute value of the diaphragm radius, thickness, and material; and of the electrode radius. However, the volume sensitivity varies inversely with the absolute value of the initial air gap. This result suggests that the air gap be designed and constructed with as small a value as is practicable in those gauge applications in which the volume change is desired minimal.

There are two alternative ways of calculating the absolute pressure sensitivities; the equations are given as items 23 and 23a in Table II. The first method (item 23) in the stiff-plate case involves knowing at least two of the elastic constants of the material of the diaphragm (Table I, item 14; Young's modulus and Poisson's ratio) with sufficient accuracy for the design problem, and using these to calculate the deflection constant.[11] In the case of the flexible membrane, it involves knowing the value of the initial stretch tension ($G/4$, item 15, Table I) in the membrane to calculate the deflection constant.[9] It was quickly found that the literature lacks the data necessary for a highly accurate calculation of the deflection constant for a stiff plate; and that the methods of measuring or calculating the initial stretch were unsatisfactory in the case of the flexible membrane. However,

[11] R. J. Roark, *Formulas for Stress and Strain* (McGraw-Hill Book Company, Inc., New York, 1938), p. 171, Case 6.

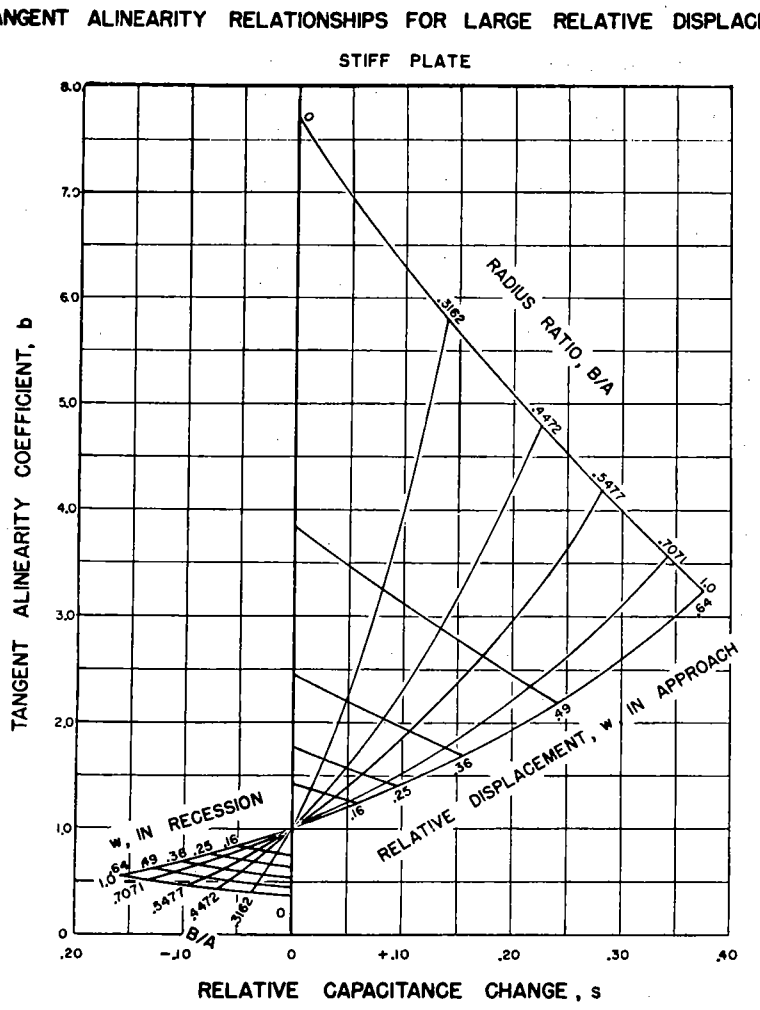

FIG. 11. The tangent alinearity coefficient for a stiff plate for large relative displacements. The tangent alinearity coefficient, b, (Table II), is defined as the ratio of the tangent relative displacement sensitivity, n, to the initial sensitivity M. A comparison of this plot with Fig. 8 shows the large deviations of the variational sensitivity (n) from linearity compared with the secant sensitivity, m.

for a first approximation in a design problem, this first method is useful.

The second method (item 23a, Table II) of calculating the pressure sensitivity envolves an independent measurement of y_0/p with a diaphragm of the desired material, thickness, and radius. Figure 14 shows such a measurement on a stainless steel diaphragm by an interferometer method. With the determined value of y_0/p, the deflection constant can be calculated (Table I) and used in further design modifications to obtain any desired c/p in an actual gauge. The data of Fig. 14 were used to calculate theoretical values of c/p in the evaluation of this design theory (Fig. 15).

EVALUATION OF THE DESIGN THEORY

Using a stiff-plate gauge shown in Figs. 16 through 19, data were taken on the pressure-capacitance performance (c/p ratios) in the approach and recession conditions (Fig. 15). To check these data against the theory, theoretical c/p values were calculated from the equation in item 23a (Table II) using the measured values of the electrode radius, B, the diaphragm radius, A, the initial capacitance, C_0, the displacement-pressure ratio, y_0/p, the value of M from Fig. 6, and the values of a from Figs. 8 and 9. The values of the y_0/p ratio were determined by an interferometric method (Fig. 14), rather than by the less accurate method of calculation from the elastic constants. The results of these calculations are plotted on the graph of Fig. 15 with the experimental data. Figure 15 shows that the stiff-plate theory can be used with a fair degree of accuracy for design purposes, even in the

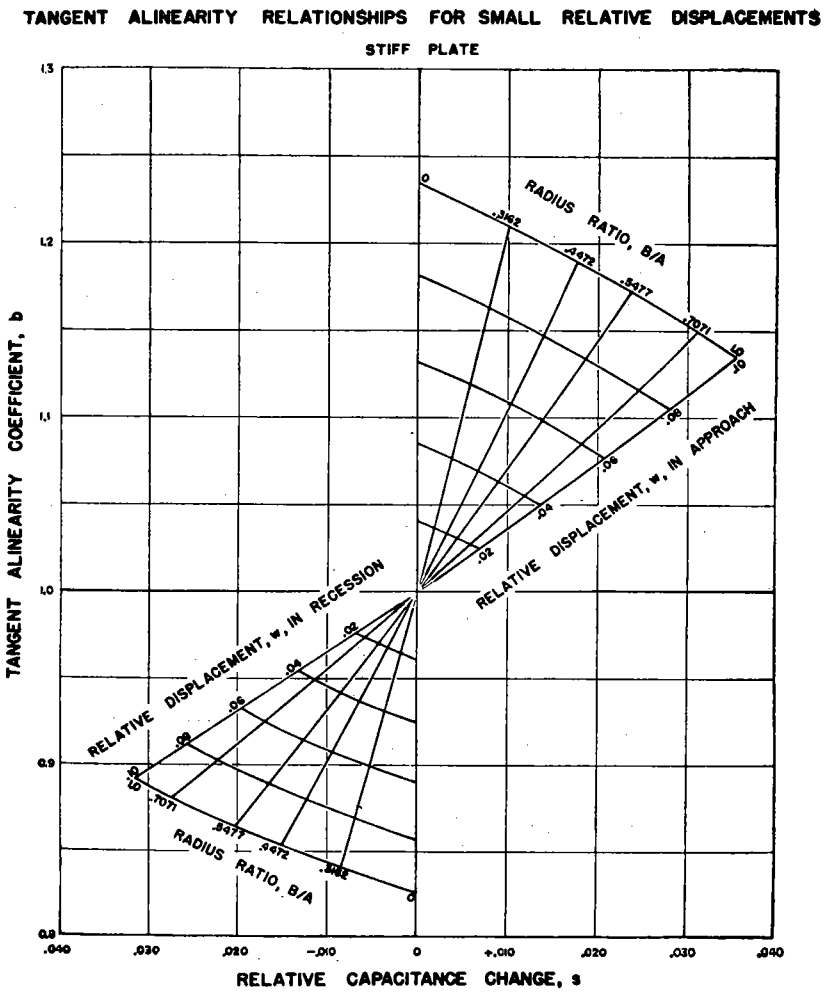

FIG. 12. The tangent alinearity coefficient for a stiff plate for small relative displacements. This plot is an enlarged view of Fig. 11 near the relative displacement of zero magnitude. This is a companion figure to number 9 for designs involving a high degree of linearity.

extreme cases involving large relative displacements ($w = \pm 0.49$) in approach and in recession. The flexible membrane theory still awaits confirmation; it is hoped that this can be done and reported in the near future; there are a few unpublished data which show that reasonably accurate predictions of performance can be expected from the flexible membrane theory.

SPEED OF RESPONSE OF A CONSTRUCTED GAUGE

Figure 20 shows the response of a gauge with an attached needle to a sudden drop in pressure level. Details of the technique of obtaining the records is given under the figure; the gauge itself is pictured in Figs. 17, 18, and 19. These records show the importance of having a homogeneous conducting medium between the source and the gauge diaphragm. They also show that fairly high speed pressure recording can be accomplished through small conduction tubing with a relatively incompressible fluid, if the volume change of the gauge is small and if the tubing wall is relatively stiff. The volume change (Table I) for the full pressure range in Fig. 20 is approximately 2×10^{-5} cc. The contained liquid volume is 0.4 cc; therefore an additional 20 percent must be added to the gauge volume change to allow for the compression of the contained water at a pressure of 150-mm Hg above 1 atmosphere.

For the speed of response of the gauge without an attached fluid system it was found that it was difficult to obtain a step change in pressure level sufficiently fast to approach the lowest natural mode of vibration of the stiff-plate diaphragms used (10 to 60 kilocycles). However, the applica-

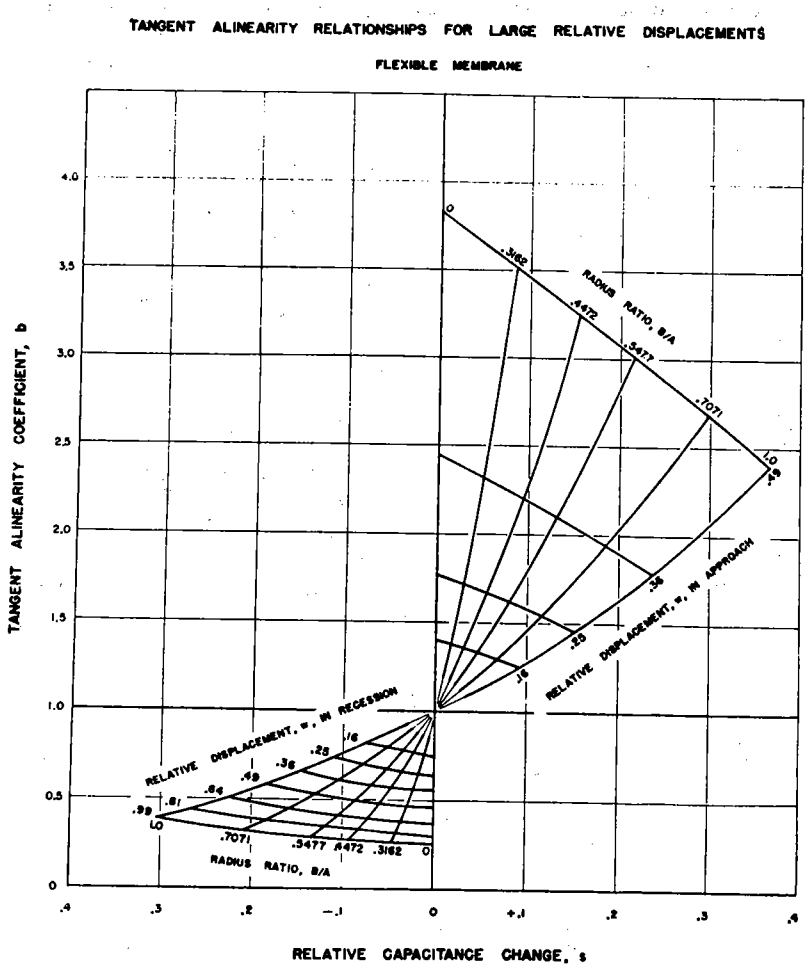

FIG. 13. The tangent alinearity coefficient for a flexible membrane. This figure is to be compared to Fig. 11 for a stiff plate. The tangent alinearity coefficients of the two cases do not differ to a great degree, in contrast to the secant alinearity coefficients (Figs. 8 and 10).

tions of the gauge to date have not made full use of the available speed of response.

CONSTRUCTION DETAILS TO OBTAIN SMALL AIR GAPS

Standard machining is performed on all components (Fig. 16) except those having critical surfaces which require special techniques as follows:

In the electrode barrel assembly, the electrode (2, Fig. 16) and its lava insulators (6) are assembled to the barrel (4) with bakelite laquer, riveted (12, Fig. 17) and baked. This assembly is faced in the lathe and hand-lapped on a plate-glass lap, until the face of both the electrode and its barrel are in the same flat plane. The electrode spacing is generated by hand-lapping the electrode face with a brass lap. The amount of spacing thus generated is gauged by placing the assembly against a flat metal gauge block and measuring the electrical capacitance between the electrode and the gauge block. If the desired spacing is exceeded, correction may be made by lapping the face of the barrel on the plate glass.

For a given diameter, diaphragms are handled differently as they vary in thickness. A diaphragm of $\frac{11}{16}$″ outside diameter could be classified thick if it were 0.008″ and over, medium 0.004″ to 0.008″, thin 0.004″ and under.

Thick diaphragms are machined from bar stock and hand-lapped to size on plate glass. Frequent turning of the diaphragm, exposing first one face then the other to the lap, will minimize warping from strain release. The thickness of the diaphragm is gauged with a micrometer. The flatness is checked by optical means or by substituting the diaphragm for the gauge block in the capacitance test described above.

Medium diaphragms are disks cut from polished, hard rolled strip metal of the required thickness. The disks are generally curved in a cylindrical plane but approach a flat surface when clamped in position.

Thin diaphragms are disks cut from polished, half-hard rolled metal of the desired thickness. They require stretching while clamping to present flat surfaces. The stretching mechanism (not shown) consists of a recess in the electrode barrel face into which the diaphragm is pressed by a ring member. The ring member is designed with clearance to insure positive seating of the diaphragm.

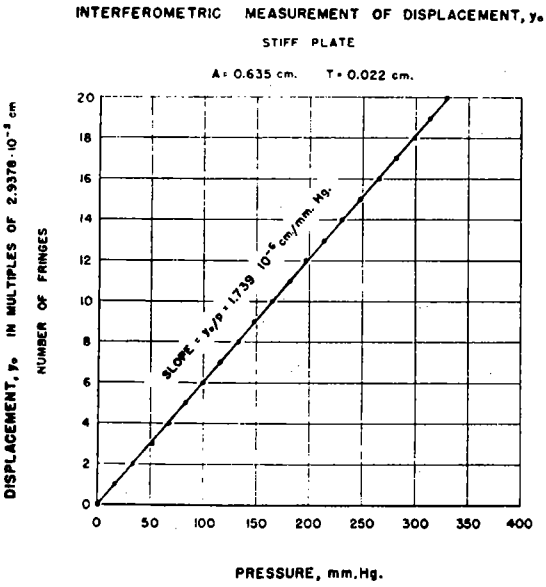

FIG. 14. Experimental determination of the pressure-displacement relation for a stiff plate. The plate is edge-clamped, and corresponds to the diaphragm of the type shown in Fig. 2. The capacitance-pressure relations for this unit are presented in Fig. 15, and the unit itself in Figs. 17, 18, 19, and 20. The absolute central diaphragm displacement, y_0 (Table I) was measured with a vertical incidence Newton's fringe type of interferometer, using a yellow line (5875.6 Angstroms) of a helium discharge tube. The fully aluminized plate (1×3×3 mm) of the interferometer was moved toward the 60 percent aluminized fixed plate by displacement of the diaphragm's center by an applied pressure. The pressure was measured with a compensated mercury manometer with an accuracy of ±0.1 mm Hg. The fringes were counted by means of a microscope and an eyepiece scale. Each fringe counted represents a movement of the diaphragm center of one-half of a wave-length of the He line, given on the left of the figure. The pressure range usually used with this gauge unit is that represented by the first two fringes, or 30 mm Hg. The diaphragm displacement is away from the electrode, i.e., in the recession condition.

The strict proportionality between the displacement and the applied pressure up to at least 300 mm Hg (ten times the range actually used) shows that this diaphragm is operated well inside of the proportional elastic limit.

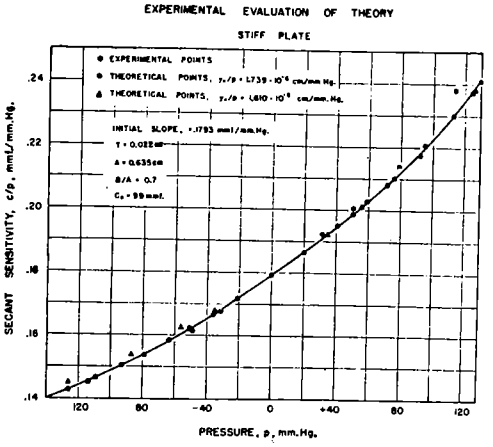

FIG. 15. An experimental evaluation of the design theory for a stiff plate. The capacitance change, c, and the initial capacitance, C_0, were measured with a "Q" meter at a frequency of 3.0 megacycles and by substitution of a precision condenser (General Radio Company). The pressure was measured with the Hg manometer mentioned under Fig. 14. The absolute pressure secant sensitivity factor, c/p, was calculated from the measured values of c and p; the solid dots and the drawn curve represent these experimental data. The dotted circles are theoretical points calculated from the value of the recession state y_0/p given in Fig. 14, the B/A value of 0.7 (measured B and A), the C_0 value of 99 mmf, the M value of Fig. 6, and the secant alinearity coefficient values of Fig. 8, by means of the equation given as item 23a in Table II. It can be seen that in recession these points fit the experimental curve fairly well, but deviate from the curve in the high pressure region in the approach state. It was then found, by the interferometric method of Fig. 14, that the value of y_0/p in the approach direction was smaller than in recession (value given in this figure). The points calculated with this value of y_0/p are the triangles. Presumably the difference of y_0/p in the two directions is due to unsymmetrical clamping supports on the two sides of the plate.

The main body (3, Fig. 16) has an interior seat against which the diaphragm is clamped. This seat is hand-lapped to a flat surface with a formed brass lap. The exterior faces of the main body are hand-lapped on plate glass to present flat seats to the mating attachments (13 and 15, Fig. 17), which are similarly finished.

All lapping operations referred to above were performed with a fine grain abrasive and light oil. Silicon carbide No. 400B was used for coarse grinding and No. 600B for finish.

ELECTRICAL CIRCUITS FOR USE WITH THE GAUGE

The circuit actually used with these gauges will be published later. The choice of a given

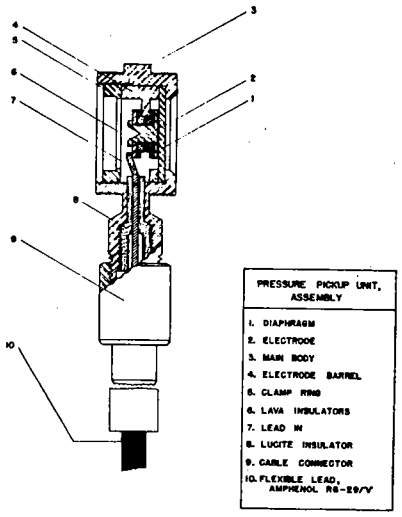

FIG. 16. Sectional drawing of a variable capacitor. The active diaphragm (1) diameter is 0.50 inches. The radius ratio B/A is 0.70. The electrode-diaphragm air gap is 5.10^{-4} cm. (0.0002 inch). The pertinent parts are labeled in the figure. The lead-in (7) carries the r.f. voltage to the electrode; the rest of this unit is grounded. It is to be noted that the electrode side of the diaphragm is kept as open as possible to allow quick venting of the gas in this space in applications in which large ambient pressure changes occur, such as in the explosive decompression of pressurized aircraft cabins in altitude chambers. The lava insulators (6) are supported by three equally spaced legs protruding inward radially from the electrode barrel (5); only one of these legs shows in this section. This construction allows the quick venting mentioned above. The construction details to assure small air gaps are given in the text.

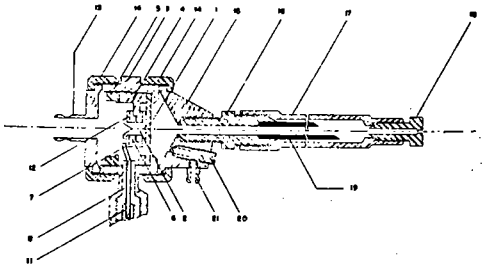

FIG. 17. Sectional drawing of a capacitor with an attached liquid system. Through number 8, the parts are the corresponding ones of Fig. 17. Photographs of this unit are shown in Figs. 18 and 19. A tubing attachment (13) for pressure calibration purposes is shown fastened to the electrode side of the unit by the retaining ring (14). A liquid system (15) with an attached hypodermic needle (16 and 19) is fastened to the diaphragm side of the unit. For the sake of clear reproduction the needle is greatly enlarged; the true relative size is shown in Fig. 18; a side tube (21) and a needle valve (20) are used for filling the liquid system. A needle guard (17) and its terminal plug (18) keep the needle wet and sterile until ready for use. This type of unit has been used for blood pressure, intrathoracic pressure and intraspinal pressure recording (Figs. 21 through 24); its response is shown in Fig. 20.

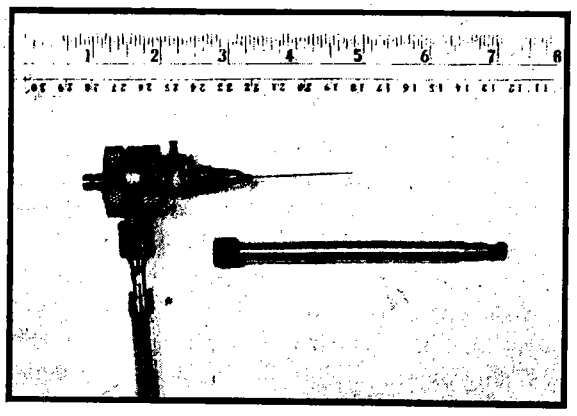

FIG. 18. Internal body pressure condenser gauge. A cross section drawing of this unit and its details is shown in Fig. 17. A photograph of this unit and its attachments is given in Fig. 19. The needle guard is below the needle. This unit is used for blood pressure and other internal body pressure recording (Figs. 23 and 24).

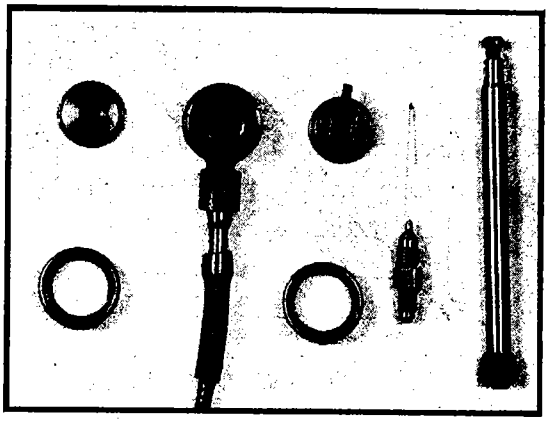

FIG. 19. Pressure gauge with attachments. This is the gauge of Fig. 18 with the tubing connector (left), the liquid system, the needle and its guard (right), removed. The one-half-inch diameter active diaphragm surface is seen as a central ring on the face of the pickup unit. All parts and the gauge itself are made of stainless steel.

circuit depends on the application; several satisfactory ones have been published.[8, 9, 12, 13] One requirement for biological work is that the electrical system record sustained capacitance changes, i.e., record the direct current component as well as the alternating current ones. Cathode-ray oscillographs and oscillograph galvanometers have both been used with success for recorders.

[12] D. W. Dana, Rev. Sci. Inst. 5, 38 (1934).
[13] C. H. Brookes-Smith, J. Sci. Inst. 16, 361 (1939).

APPLICATIONS OF THE GAUGE TO MECHANICAL MEASUREMENTS IN BIOLOGICAL SYSTEMS

Various applications of the gauge to pressure recording during the war are presented in Figs. 21 through 25. Since the applications are described under the figures, no further comments will be made here. Other uses of the gauge as an ultramicrometer or a dilatometer in biological systems might be mentioned. The gauge may be used to measure the movements of the body resulting from recoil caused by heart and blood motions in an electrical ballistocardiograph. An obvious use is as a high speed, isometric "lever" for recording the tension developed by muscles during fast or sustained contractions; it may be possible to use it for single muscle fibers. As a dilatometer, the gauge can be used in plesthysmography, thermometry, and respirometry. The volume changes in muscle during fast contractions may possibly be recorded. It may be used in the measurement

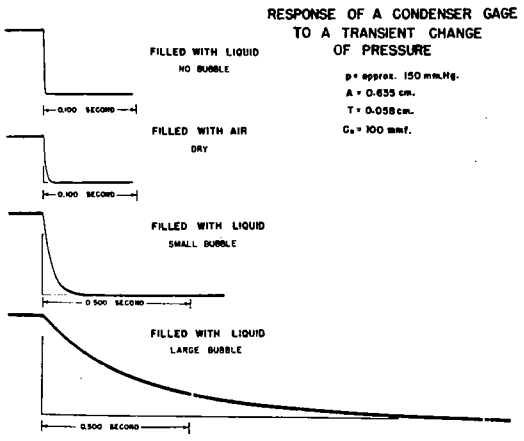

FIG. 20. Response of a capacitor gauge with attached needle to a sudden fall in pressure level. The gauge itself is of the type shown in Figs. 18 and 19. The attached hypodermic needle was a number 23, one-inch long. The volume of the liquid system is 0.4 cc. The needle was immersed in liquid or in air in a short $\frac{1}{2}$-inch diameter well in the face of a 6-inch diameter, horizontal plate, over which was stretched a thin paper diaphragm. The pressure in the air space between the plate and the paper diaphragm was raised with an air supply, and the paper diaphragm was "exploded" away with a mouse trap lever traveling at high speed. The paper broke completely away over the whole plate surface, causing a rapid fall in pressure over the well containing the needle. The conditions causing the various rates of fall of the gauge response are given in the figure. The top record shows a response time of about one-thousandth of a second, which is an upper limit, presumably set by a time constant in the electrical circuit used for recording, rather than by the response time of the mechanical system. (To fill the system with liquid without bubbles, the contained air was flushed out with pure carbon dioxide gas before filling; any bubbles formed of CO_2 quickly dissolve in the liquid, leaving the system completely liquid filled.)

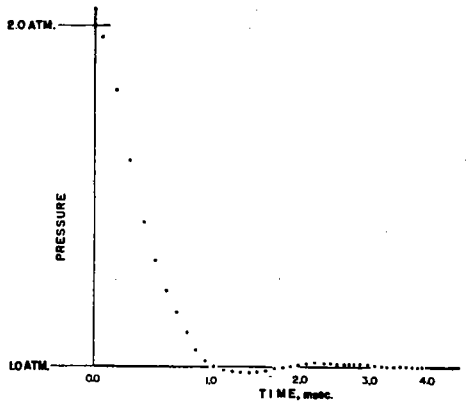

FIG. 21. Explosive decompression of a short cavity. The condenser pressure gauge (of the type shown in Fig. 17) was placed in the bottom of a well 3 inches long and $\frac{3}{4}$-inch in diameter and containing air. By the technique described under Fig. 20, the pressure at the mouth of this well was suddenly dropped to the ambient pressure from twice the ambient value. This retouched record of the pressure was photographed on a cathode-ray oscilloscope. The time between dots is one ten-thousandth of a second. Note the relatively small after-vibrations in contrast with those of Fig. 22. This gauge was subsequently used in recording the pressure fall in explosively decompressed pressurized cabins in an altitude chamber; the minimum time of pressure fall recorded in these cabins was about four times the value shown here.

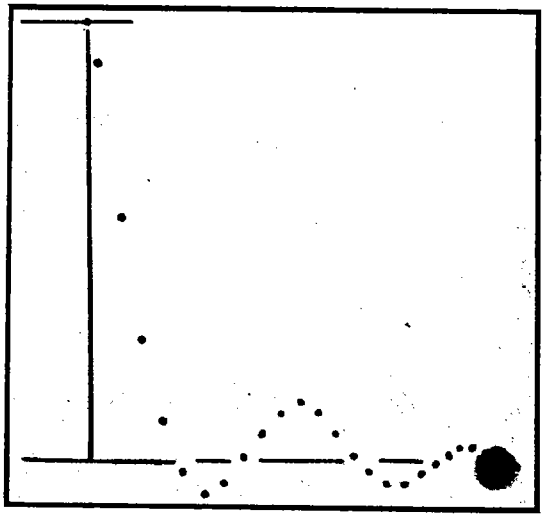

FIG. 22. Explosive decompression of a long air cavity. The technique and the pressure range are the same as those of Fig. 21. The $\frac{3}{4}$ inch diameter cavity in this case, however, is 3 feet long. The time between dots is two ten-thousandths of a second. The amplitude of the first after-vibration is 2.0 pounds per square inch, after an initial fall of 15 pounds per square inch. This record shows some of the artifacts created by trying to measure relatively large rapid changes in pressure through a long pressure lead, filled with air.

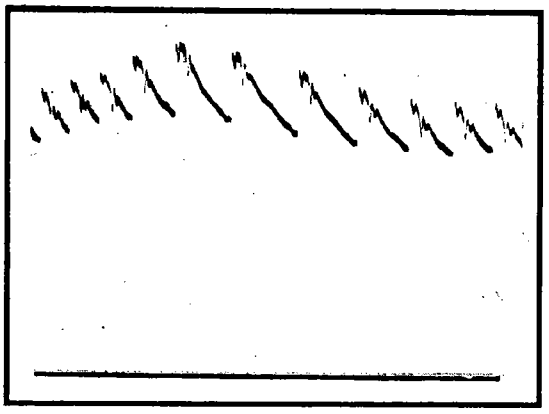

FIG. 23. A blood pressure record in the carotid artery of a dog. The pressure base line is at the bottom of the figure. The peak pressure is approximately 150 mm Hg. The record was taken with a pressure gauge of the type shown in Figs. 18 and 19. This record is shown through the kindness of H. C. Bazett.

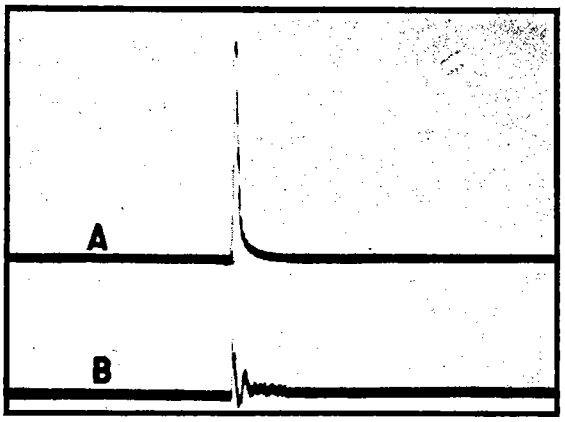

FIG. 24. Record of the intrathoracic and the intraspinal pressure in an explosively decompressed dog. *A* is the intrathoracic pressure record, and *B* the intraspinal pressure record. The breaks in the falling phase of record *A* are at 1/120 second intervals. The condenser gauge used was of the type shown in Figs. 18 and 19. The dog was in a small chamber at an equivalent pressure of 8000 feet; a thin film diaphragm separated this chamber from a larger one at a lower pressure. When the diaphragm was ruptured, the air pressure around the dog fell in 0.03 seconds to that equivalent to 50,000 feet. The two gauge pick-up units were liquid filled, with an electrode side open to ambient pressure and its changes (Fig. 16). The needles were in their respective body spaces. The pressure rise with respect to ambient (about 30 mm Hg in *A*) is apparently due to the relative delay of the air flowing from the lungs. This figure is reproduced through the courtesy of Fred A. Hitchcock, Ohio State University.

of the stimulus of nerve or muscle when pressure or mechanical stresses are applied in a slow or

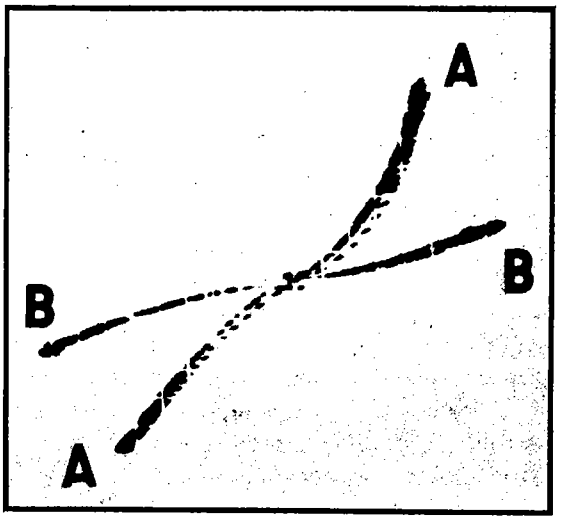

FIG. 25. Pressure-flow curves for air through the nasal passageway. Two, flexible membrane-type pressure gauges with a pressure range of 100 mm of water and 10 mm of water for a capacitance change of 5 mmf were used for recording air pressure and air flow, respectively. The record is a photograph of a cathode-ray tube screen, with flow appearing on the horizontal axis and pressure on the vertical axis. Zero flow and zero pressure are at the center of the record where the two lines cross. Expired gas flow and pressure are in the right upper quadrant, inspired values in the lower left one. The flow values cover about ±50 liters/minute; the pressure about ±80 mm of water. The flow is recorded by measuring the pressure drop across a laminar-flow type glass wool resistor, placed in the tube exit from an oxygen mask covering the subject's nose and mouth. The pressure was measured differentially between the inside of the mask and in *A–A*, the subject's oropharynx, and in *B–B*, his nasopharynx. In both cases, one nostril is plugged; in *A–A* the pressure tap tube goes into the mouth; in *B–B* the tube goes through the plugged nostril. Record courtesy of Forman and Benevides.

in a fast manner. It is hoped that the design theory presented above will be an aid in extending the applications of this type of gauge in biological research and in the engineering and physical fields.

ACKNOWLEDGMENTS

The authors wish to express their thanks to Dr. D. W. Bronk for his encouragement during the course of this work; to A. J. Rawson and J. P. Hervey for their help and suggestions; and to J. R. Pappenheimer and G. A. Millikan for their stimulating applications for this gauge.